“The 1st international symposium on VLEO missions and technologies”
June 28-29,2021, Manchester, UK

Molecular scattering at microstructured surface for rarefied gas compression inside air breathing ion engine

Kosuke SHODA, Naoki KANO, Yuki JOTAKI, Keisuke EZAKI, Kazuki ITATANI, Takashi OZAWA*, Yusuke YAMASHITA**, Kazutaka NISHIYAMA, Kumiko YOKOTA and Masahito TAGAWA***

Department of Mechanical Engineering, Kobe University, Rokko-dai 1-1, Nada, Kobe 657-8501, Japan
**Japan Aerospace Exploration Agency, Jindaiji-Higashimachi 7-44-1, Chofu, 182-8522 Japan*
***Department of Aeronautics and Astronautics, University of Tokyo,*
Yoshinodai 3-1-1 , Chuo-ku, Sagamihara, Kanagawa 252-5210, Japan
****Institute of Space and Astronautical Science, Japan Aerospace Exploration of Agency,*
Yoshinodai 3-1-1 , Chuo-ku, Sagamihara, Kanagawa 252-5210, Japan

Corresponding authors: Kosuke Shoda (201t336t@stu.kobe-u.ac.jp)
Masahito Tagawa (tagawa@mech.kobe-u.ac.jp)

1. Introduction

Utilization of low-altitude satellites are expanded rapidly on Earth observation, navigation and communications in recent years. It has been recognized that high-resolution observations and low-energy communications are realized by orbiting lower altitudes called very low Earth orbit (VLEO) or sub-LEO. However, the atmospheric drag prevents a satellite to descend lower than 300 km without propulsion systems. Recent attempts to operate satellites in VLEO such as Examples include Gravity Field and Steady-State Ocean Circulation Explorer (GOCE) [1] and Super Low Altitude Test Satellite (SLATS) [2] used electric thrusters to compensate the atmospheric drag. The mission lives of these satellites were limited by the amount of Xe on board. For longer operation of satellite in VLEO environment requires large Xe tank which leads to increase the atmospheric drag.

To break this chain reaction of negativity, idea of propellant correcting thrusters have been considered from 1960s by many researchers [3-4], however, never became realistic. However, a significant progress on propellant correcting thruster concept was made by Nishiyama in 2003 [5]. Air breathing ion engine (ABIE) integrates the high-efficiency passive compression intake system and ECR ion engine. This ECR ion engine system was applied to Hayabusa and Hayabusa-2 planetary probes and exhibits high performance and reliability [6]. Therefore, unsolved problem is the design of high-efficiency passive compression intake system.

An original high-efficiency passive compression intake was experimentally tested by Tagawa et al [7]. The use of fine collimator allows flow-in hyperthermal directional molecules from outside the inlet and prevents flow-out randomly moving molecules with thermal velocity through collimator. The effect of collimator to prevent the back streaming molecules were experimentally verified. An important point of the intake design is to achieve the maximum conductance of incoming flow and the minimum conductance of outgoing flow in the intake. The collimator system tested in [8] uses the difference in moving directions of molecules; however, scattering event at collimator surface is isotropic on both moving directions. In this study, we evaluate the effect of microstructure on the collimator surface to achieve anisotropic scattering properties. DSMC calculation was performed to evaluate the compression performance of the microstructured intake system based on the results of molecular scattering experiments.

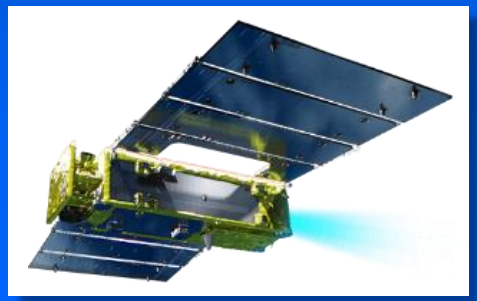

Figure 1 Super Low Altitude Test Satellite (SLATS)

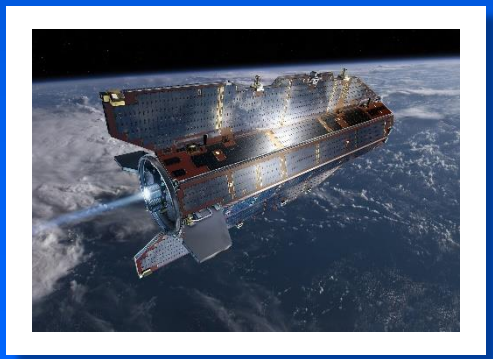

Figure 2 Gravity Field and Steady-State Ocean Circulation Explorer (GOCE)

Figure 3 Hayabusa-2

2. Molecular Scattering Experiments

Schematic diagram of the experimental apparatus is shown in Figure 4. This is the same facility used in the first ignition experiment in 2009 [8]. The experimental facility consists of three vacuum chambers, which are referred to as the source, reaction and time-of-flight (TOF) chambers from the upstream. Molecules beam pulse are formed by the pulsed supersonic valve (PSV) attached to the source chamber [9]. The PSV is capable of ejecting gas pulse with thermal velocity at typically 3 Hz. Gas pulse is introduced to the reaction chamber with a 3 mm skimmer. The sample is mounted on the inner rod of the coaxial θz stage, whereas the MG-2 ionization gauge is mounted on the detector arm attached to the outer rotatable cylinder located in the reaction chamber (Figure 5). A filament and a grid of the MG-2 ion gauge are controlled by the original electronics, however, ion current from the ion collector is directly measured by a digital storage oscilloscope after amplified by a fast IV preamplifier. Figure 6 shows typical TOF spectrum recorded by the digital oscilloscope. Measurement signal was accumulated for 400 pulses, and clear signal by scattered molecules are detected. A laser-detonation system has capability to form hyperthermal beams pulses at orbital velocity of spacecraft (8 km/s), the experiment was performed by thermal beam pulses because most of the molecules in the intake are thermally equilibrium.

Figure 7 shows a SEM photograph of the microstructured surface tested in this experiment. One directional groves with triangle cross-section are formed in the sample surface. The surface was covered by the facet structure at 20 and 74 degrees. Top most surface was coated by Au layer. Au flat mirror was also used for comparison purpose. Detail of the sample is listed in Table 1. All scattering experiments were carried out by thermal Ar beam pulses. Experimental conditions are listed in Table 2.

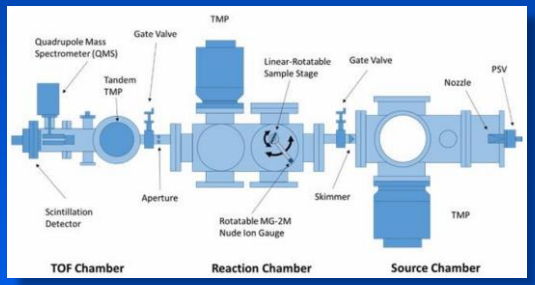

Figure 4 Schematic drawing of the experimental facility used in the rarefied gas scattering experiment.

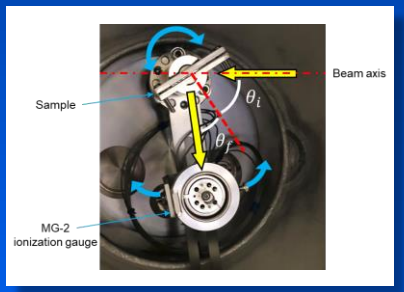

Figure 5 MG-2 ionization gauge and sample mounted on the coaxial zθ stage. Incident and final angles and defined as shown in the figure.

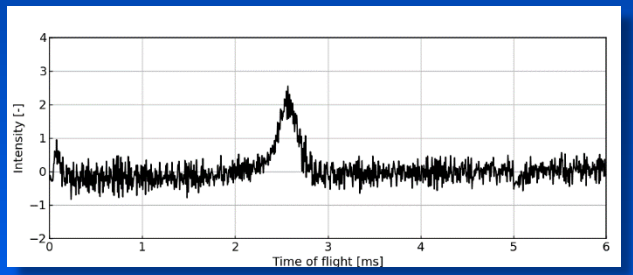

Figure 6 Typical TOF spectrum recorded on the digital storage scope.

Table 1 Samples used in this study

Incident species	Ar
PSV pressure (Pa)	35?
Distance between PSV and sample (mm)	1250
Distance between sample and ionization gauge (mm)	70
Base pressure (Pa)	3E-7
Repetition rate (Hz)	3
Sample temperature	room temp.

Table 2 Experimental conditions

	Au-coated mirror	Microstructured surface
Surface coating	Au	Au
Substrate material	Cu	Float glass
Facet angle (degree)	-	20
Facet angle (degree)	-	74
Cyclic period (mm-1)	-	830
Size and shape	25 mm in dia.	25 x 25 mm in square

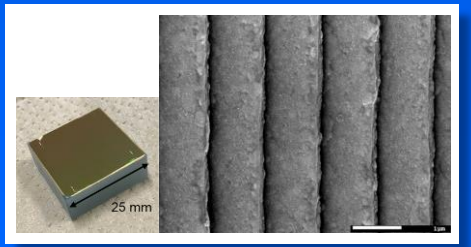

Figure 7 Photograph and SEM image of the microstructured surface. The facet angles are 20 and 74 degree and the period length is 1 μm.

3. Experimental Results

Figure 8 shows the flux distributions on the Au-coated flat surface. The measurement was performed at the incident angle at 0, 30 and 60 degrees. Scattering distributions at the incident angles at 30 and 60 degrees indicate lobular distributions. In contrast, the scattering molecules at normal incidence showed combined distribution of diffuse and lobular patterns. It was observed that the Au surface used in this experiment shows a lobular distribution rather than diffuse pattern.

Figure 9 shows the flux distributions at the Au-coated microstructured surface. The measurement was performed at the macroscopic incident angle at 0, 30 and 60 degrees against the substrate (not a facet). In Figures 9(a) and 9(d), scattering patterns are similar to the diffuse scattering and no lobular component is observed (see Figure 8(a)). In contrast, one can find that clear lobular distribution is observed in Figure 9(c). Because the facet normal is -20 degree, the microscopic incident angle to the facet surface is 40 degree and the specular reflection locates at +20 degree in Figure 9(c). This angle agrees well with the results observed. Thus, the reflection pattern in Figure 9(c) is explained by the simple lobular scattering similar to that observed at the flat Au surface in Figure 8. In Figure 9(e) small hump is obvious at close to the specular direction of the facet (-50 to -60 degree). On the other hand, almost similar reflection flux is measured in the region from -30 to +30 degrees. This is probably due to the diffuse component of the scattering. The rapid decrease at -60 degree in Figure 9(e) is probably due to the shadowing effect by the neighbor facet. The effect of neighbor facet is also observed in Figure 9(f) which is grazing angle incidence case. The microscopic incident angle to the facet surface is 80 degree in Figure 9(f) and forward scattered molecules collides with the edge of the neighbor facet. Or major part of the incoming molecule directly collides to the edge of the facet. As a result, large signal is observed in the backscattering region. The scattering distribution in Figure 9(b) is difficult to explain. It is close to the normal incidence on facet from the microscopic point of view, and effect of multiple bounce hardly occurs in this configuration. However, overall scattering pattern seems to be a very wide lobular distribution regarding the macroscopic incident angle. This is due probably to the complex nature of scattering at the microscopic structures.

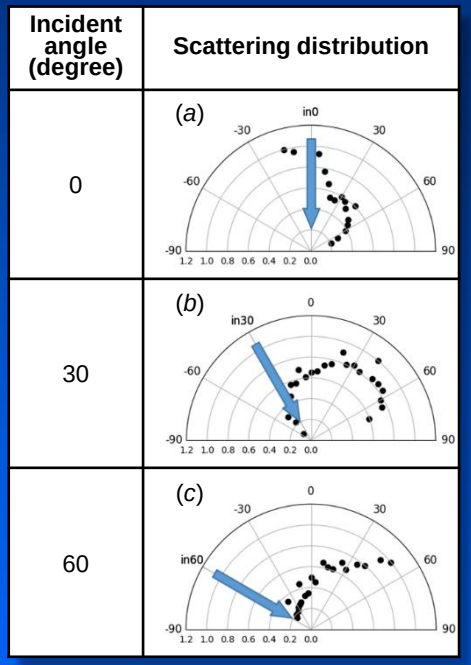

Figure 8 Flux distributions of thermal Ar beam scattered on the Au-coated flat surface at room temperature. Blue arrows show the directions of the incident beam.

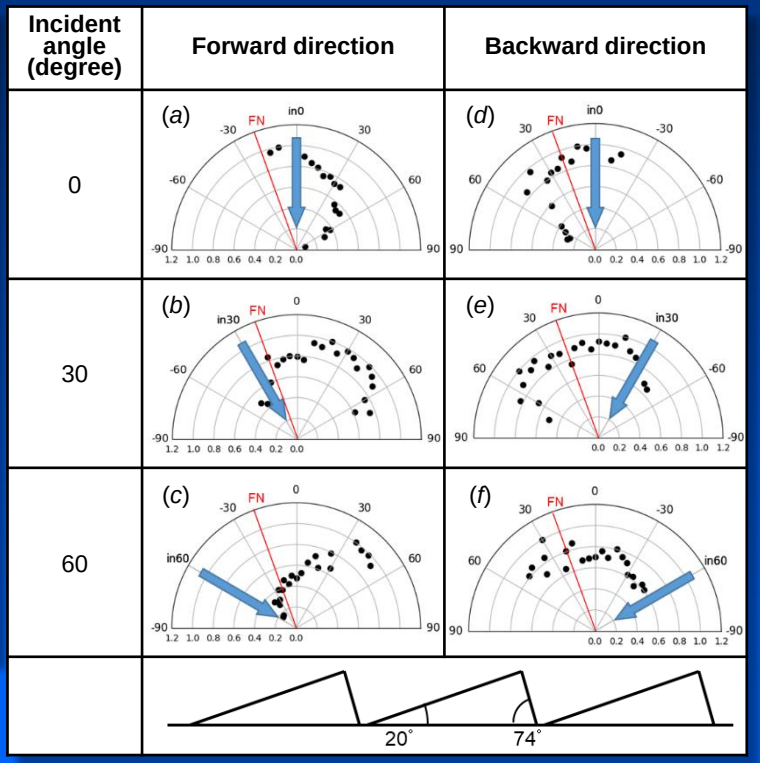

Figure 9 Flux distributions of thermal Ar beam scattered at the Au-coated microstructured surface at room temperature. Blue arrows show the directions of the incident beam and FN represent the direction of the facet normal. The direction of the microstructure is indicated at the bottom of the figures.

4. DSMC Simulation on Compression Performance

From a series of scattering experiment, the complex scattering properties of microstructure surface is observed. It is summarized as follows: when the incident angle is large in forward direction, the scattered molecules are distributed mainly in the lobular pattern regarding the facet surface. On the other hand, when the incident angle is small in positive direction and all negative directions, the scattering distribution does not have a specific peak, but indicate rather diffusive reflection. In order to evaluate the unique scattering property of the microstructured surface on the compression performance of intake system for ABIE, Direct Simulation Monte Carlo (DSMC) method was applied. According to the results of the scattering experiment, a scattering model which combines the specular and diffuse reflection schemes is used in the DSMC calculation: incident molecules which have macroscopic incident angle between +90 and -20 degrees follow the diffusive scattering, however, those have incident angles between -20 (FN direction) to -90 degrees do the specular scattering as shown in Figure 10. The double cylindrical ABIE model proposed by Ozawa is used in this calculation (Figure 11). The molecules are collected from the intake left side of the figure, and compressed the spaces between the inner and outer cylinders. Molecules reach the end of the compressed region are reflected to the accommodation cavity and are introduced to the discharge chamber. The conditions used in the DSMC calculations are shown in Table 3. The compression performance is evaluated by the compression ratio G which is defined by the ratio of number densities in the discharge chamber (n_{dis}) and those in outside of ABIE (n_{atm}).

$$G = \frac{n_{dis}}{n_{atm}}$$

Calculations are performed in two cases: (1) intake surface is covered by the microstructured surface and (2) is cover by normal surface with 100% diffuse scattering scheme. Table 4 shows the calculation results. By applying the microstructured surface to the intake surface, the compression ratio increases to the by about 186.6, which is 28 % greater than the 100% diffusive flat surface. Note that the result is obtained with rough DSMC modeling and non-optimized shape and material of the microstructure. The optimization of the shape such as facet angle, surface material and DSMC modeling will provide better and accurate results on compression performances of ABIE intake.

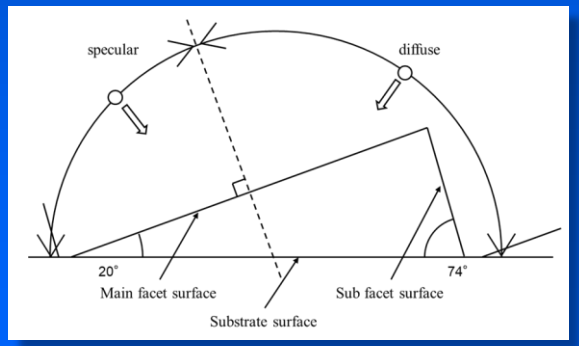

Figure 10 Reflection model used in the DSMC calculation

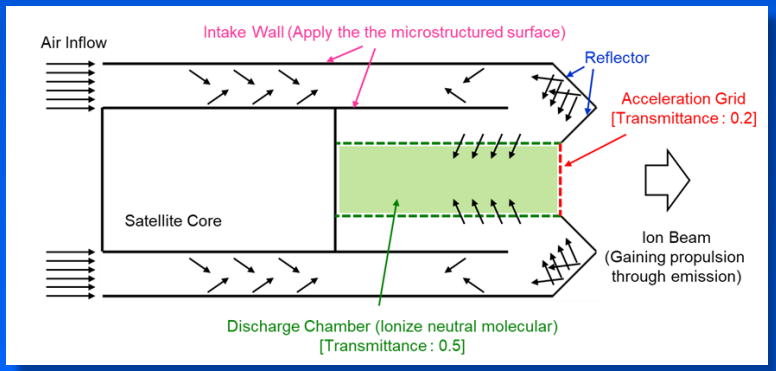

Figure 11 Double cylindrical ABIE

Table 3 Simulation conditions

ABIE model	Double cylindrical type
Altitude (km)	250
Number density (m-3)	1.43×10^{15}
Inflow velocity (m/s)	7754
Atmospheric temperature (K)	839.6
Wall temperature (K)	300.0
Gas-surface interaction model except intake surface	Diffuse
Mass of molecule (Kg)	3.26×10^{-26}
Transmittance	0.5 (discharge chamber) 0.2 (acceleration grid)

Table 4 Compression performance simulated by DSMC

Microstructured intake	Flat intake
186.6	145.9

5. Conclusions

The effect of microstructure surface on the passive compression performance of the intake system of air-collecting thruster system was proposed and demonstrated. Scattering distribution of thermal Ar beam pulse was measured experimentally and anisotropic nature of scattering was confirmed. Scattering process at the microstructure surface is complex due to multiple bounce effect at the facet surface even though each scattering is similar to that at flat surface. DSMC calculation at the condition of 250 km in altitude was performed using the simple scattering model which was based on the experimental results and ABIE design. It was observed that the compression performance increased 28 % compared to the normal surface. The optimization of the shape and material of microstructure will provide better compression performances of ABIE intake system.

Acknowledgments

A part of this study was supported by the KAKENHI from JSPS under contract #18H01624, #18K18912, #19H02346 and #19K22017.

References

[1] GOCE home page; http://www.esa.int/Our_Activities/Observing_the_Earth/GOCE
[2] Imamura, S., Utashima, M., Ozawa, T., et al., "Current status of the on-going orbit transfer of super low altitude test satellite (SLATS)", In: Proceedings of the 69th International Astronautical Congress, IAC-18-C1.8.1. Bremen, Germany, 2018
[3] Cara D., Amo G., Santovincenzo A., et al., "RAM Electric Propulsion for Low Earth Orbit Operation", an ESA Study, IEPC-2007-162, 2007
[4] Cifali G., Misuri T., Rossetti P., et al., "Experimental characterization of HET and RIT with atmospheric propellants", in Proceedings of 32nd International Electric Propulsion Conference, Wiesbaden, Germany, 2011, IEPC-2011-224
[5] Nishiyama K., "Air breathing ion engine concept", in: Proceedings of the 54th International Astronautical Congress of the International Astronautical Federation, the International Academy of Astronautics, and the International Institute of Space Law, Bremen, Germany, 2003, IAC-03-S.4.02, doi: 10.2514/6. IAC-03-S.4.02.
[6] Coral G., Tsukizaki R., Nishiyama K., et al., "Microwave power absorption to high energy electrons in the ECR ion thruster", Plasma Sources Science and Technology, 2018, Vol.27, No.9
[7] Tagawa M., Nishiyama K., Yokota K., et al., "Experimental Study on Air Breathing Ion Engine using Laser Detonation Beam Source", J. Propulsion and Power, Vol.29 (2013) 501-506.
[8] Tagawa M., Nishiyama K., Yokota K., et al., "An experimental study on air breathing ion engine using a laser-detonation atomic oxygen beam source as LEO space environment simulator", The 27th International Symposium on Space Technology and Science, Tsukuba, Japan, 2009.07.05-07.12, on USB Memory.
[9] Tagawa M., Okura R., Yokota K., "Reduced Dissociation of Molecules in Laser-Detonation-Driven Hyperthermal Beams", Proc. Adv. Space Environ. Conf., Universal City USA, May 13-17, 2019